Journal of Biomedical Optics

SPIEDigitalLibrary.org/jbo

Visualization of human heart conduction system by means of fluorescence spectroscopy

Jonas Venius
Saulius Bagdonas
Edvardas Žurauskas
Ricardas Rotomskis

SPIE

Visualization of human heart conduction system by means of fluorescence spectroscopy

Jonas Venius,[a] Saulius Bagdonas,[b] Edvardas Žurauskas,[c] and Ricardas Rotomskis[a,b]
[a]Vilnius University Institute of Oncology, Laboratory of Biomedical Physics, Baublio 3A, Vilnius, LT- 08406, Lithuania
[b]Vilnius University, Laser Research Center, Saulėtekio 9, c.3, Vilnius, LT-10222, Lithuania
[c]Vilnius University Medical Faculty, Čiurlionio 21, Vilnius, LT-03100 Lithuania

Abstract. The conduction system of the heart is a specific muscular tissue, where a heartbeat signal originates and initiates the depolarization of the ventricles. The muscular origin makes it complicated to distinguish the conduction system from the surrounding tissues. A surgical intervention can lead to the accidental harm of the conduction system, which may eventually result in a dangerous obstruction of the heart functionality. Therefore, there is an immense necessity for developing a helpful method to visualize the conduction system during the operation time. The specimens for the spectroscopic studies were taken from nine diverse human hearts. The localization of distinct types of the tissue was preliminary marked by the pathologist and approved histologically after the spectral measurements. Variations in intensity, as well as in shape, were detected in autofluorescence spectra of different heart tissues. The most distinct differences were observed between the heart conduction system and the surrounding tissues under 330 and 380 nm excitation. The spectral region around 460 nm appeared to be the most suitable for an unambiguous differentiation of the human conduction system avoiding the absorption peak of blood. The visualization method, based on the intensity ratios calculated for two excitation wavelengths, was also demonstrated. [DOI: 10.1117/1.3631786]

Keywords: fluorescence spectroscopy; visualization; heart conduction system.

Paper 11077RR received Feb. 22, 2011; revised manuscript received Jul. 29, 2011; accepted for publication Aug. 8, 2011; published online Oct. 3, 2011.

1 Introduction

Various methods of the optical spectroscopy, which provide a noninvasive acquisition of the real time data, continue to gain new application areas in biomedical research and clinical diagnostics. Autofluorescence reflecting the intrinsic features of the biological tissue has become a useful parameter for the differentiation between the tissues otherwise being visually indiscernible.[1,2] The recent development of the new compact light sources, especially in the near-UV spectral region, as well as miniaturization of the fiber-optics–based registration equipment eventually creates a new boost for the fluorescence-based diagnostic techniques application during complex surgery of internal organs, such as surgery of the heart.

During the surgical intervention in the case of congenital heart diseases,[3] heart artery bypass, and valvular diseases,[4,5] there is a possibility to harm the conduction system of the heart (HCS), which may result in a dangerous obstruction of the heart functionality. The HCS is a specific muscular tissue where a heartbeat signal originates and then spreads through its branches to the different parts of the heart initiating the depolarization of the ventricles. Thus, it is absolutely vital for generating and synchronizing the heartbeat. However, due to the muscular origin of both HCS and myocardium (MC), it is complicated to distinguish these two tissues visually.

A lot of information has been collected over the last 100 years on the histological, morphological, and physiological characteristics of the specialized hearth tissues.[6] Nowadays it is known that HCS begins with the sinoatrial (SA) node, in which the depolarization of the pacemaker cells dictates the heart beat rhythm. An impulse generated in the SA node spreads through the atriums to the atrioventricular node (AV), whereas the conduction system transforms into the His bundle (HB) connecting atriums with ventricles. In the interventricle septum, HB splits into two branches which branch off in the myocardium of ventricles and end in the inner ventricular walls as thin Purkinje fibers.[7,8]

The HCS plays a totally different role from the myocardium and has different electric characteristics—an impulse through HB propagates about 10 times faster than in the myocardium.[7,9] This suggests that the respective two muscular tissues should have some qualitative or quantitative differences in their structure and/or molecular composition. The tissue specimens taken from the conduction system and ordinary myocardium of the human heart were investigated using a method of the steady state absorption spectroscopy.[10] The spectroscopic differences between the conduction system and the myocardium had been identified. The differences were conditioned by the presence of the diverse amounts of the amino acids tryptophan and tyrosine[10] in these tissues that could cause different autofluorescence intensities. Investigations of the myocardium viability by applying the fluorescence spectroscopy method revealed an intense MC fluorescence at 330 nm under excitation with a laser beam at 248 nm.[11] Perk et al.,[12] during the studies on human heart tissues, have shown that there was indeed a difference in intensity between fluorescence spectra registered from the endomyocardial and the nodal tissues. Under excitation at 337 nm,

Address all correspondence to: Jonas Venius, Vilnius University Institute of Oncology, Scientific Research Center, Baublio 3B, Vilnius, 20102 Lithuania. Tel: 37052190902; E-mail: jonas.venius@vuoi.lt.

1083-3668/2011/16(10)/107001/9/$25.00 © 2011 SPIE

the fluorescence intensity from AV and SA nodes was higher than that from the ventricular endocardium and approximately the same as from the atrial endocardium.[12] Other researchers investigated myocardial tissue of the sheep hearts and showed that atriums fluoresce more intensively than the ventricles.[13] The main fluorophores characterizing the fluorescence of the myocardial tissue were found to be collagen and elastin.[14–16] However, the visualization of the heart conduction system still remains at the primary level, and there is an immense necessity for developing a method, which would help to visualize the conduction system during the operation time.

Our previous studies[17,18] performed *ex vivo* on prepared tissues revealed that the His bundle tissue could be distinguished from the myocardium by more than a two-fold increase in intensity at wavelengths starting from 400 to 500 nm under excitation at the UVC spectral region. However, this method of differentiation is of low clinical value due to the potentially harmful biological effect of the UVC radiation. The clear difference between autofluorescence spectra has been observed in this region under the predominant excitation of collagen at 330 nm and elastin—at longer wavelengths (e.g., 366 or 380 nm). The comparison between the autofluorescence data of the connective tissue (CT) and those of the bundle of His has also revealed the possibility for the fluorescence-based differentiation between these tissues. Although the experiments were performed *ex vivo* on microscopically (histologically) prepared specimens, the preliminary macroscopic visualization has been done taking into account the obtained spectroscopic data.[17] The direct visualization of HCS by illuminating the heart at 366 nm seemed to be helpful, but it did not resolve the problem of HCS differentiation from CT, since both types of the tissue possess a much higher fluorescence intensity than MC. While the presence of the regular CT in the healthy myocardium is very unlikely, nevertheless, it could appear after surgical interventions, heart attack, or in various pathological cases,[7] thus reducing the unambiguity of the direct visualization.

In addition, the spectral properties of HCS and MC are altered by fluorescence of the endocardium (EC) tissue, which overlays the internal surface of the heart. Endocardium contains elastin and collagen fibers like the connective tissue.[9] As it was demonstrated earlier,[16–18] the connective tissue possessed the highest autofluorescence intensity. Previous studies were performed on prepared tissues without EC, therefore the fluorescence intensity of heart tissues covered by EC tissue is expected to be higher. This could lead to the reduced contrast between MC and HCS in the case of direct visualization under UV illumination.

Consequently, in our present study the characteristic features of the fluorescence and fluorescence excitation spectra (reported earlier for the endocardium free specimens) were tested to differentiate between HCS, MC, and also CT in the specimens of the heart tissue covered with endocardium. The study was also focused on the search of the spectroscopic method that would allow distinguishing between the tissues having similar fluorescence intensities such as HCS and CT and would be relatively insensitive to the different illumination levels.

2 Materials and Methods

Nine human heart samples from 9 subjects (of middle age, without heart pathology) were obtained at autopsy (12 to 24 h post mortem) by the pathologist in the National Center of Pathology. All specimens of 3 to 4 cm in size were prepared from the left branch of His bundle taken together with surrounding tissues of the human heart according to the methodology described earlier.[17] Since the hearts chosen for investigations were without pathology and there were no sites of clear fibrosis, the specimens that contained all three types of the tissue were prepared from the top part of the interventricular septum. Preparations were fixed in a 10% neutral buffered formalin solution immediately after excision and kept in the dark at 4°C. Eight of the nine samples were used for the spectral analysis and one specimen was used for demarcation and visualization of HCS.

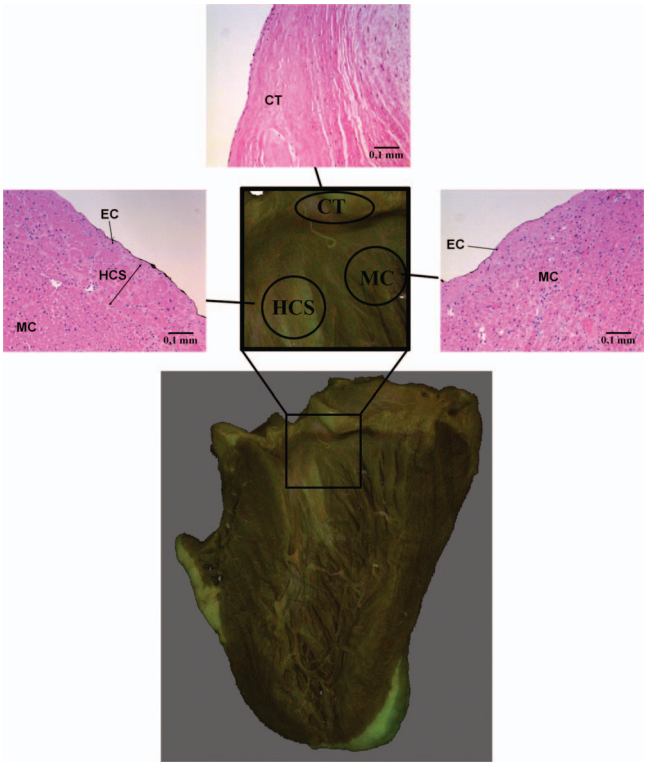

Fig. 1 Specimens were made from the healthy hearts. The localization of distinct tissues was preliminary marked (circles) by a pathologist and verified histologically after spectral measurements.

The localization areas of the distinct types of the tissue were preliminary marked by the pathologist based on anatomical features of the heart (Fig. 1). The location of HCS and MC was marked in all specimens and only in three of them some places were marked as CT. The spectral analysis of the marked places has been done by measuring fluorescence spectra on 37 spots from 8 different specimens.

While performing each experiment a picture of a sample was taken and the spots, where the fluorescence spectra had been measured, were pointed on the picture or labeled on the tissue with a pin. Pictures of the samples were taken in the daylight and under homogeneous exposure to a set of two UV lamps (peak intensity at 365 nm, full width at half maximum—20 nm).

After the spectral measurements, the spots were investigated histologically. For that, tissue samples were embedded in paraffin. Sections of 4-μm thickness were done perpendicular to the surface with the Leica RM2145 microtome and were stained by hematoxylin and eosin according to an ordinary histology

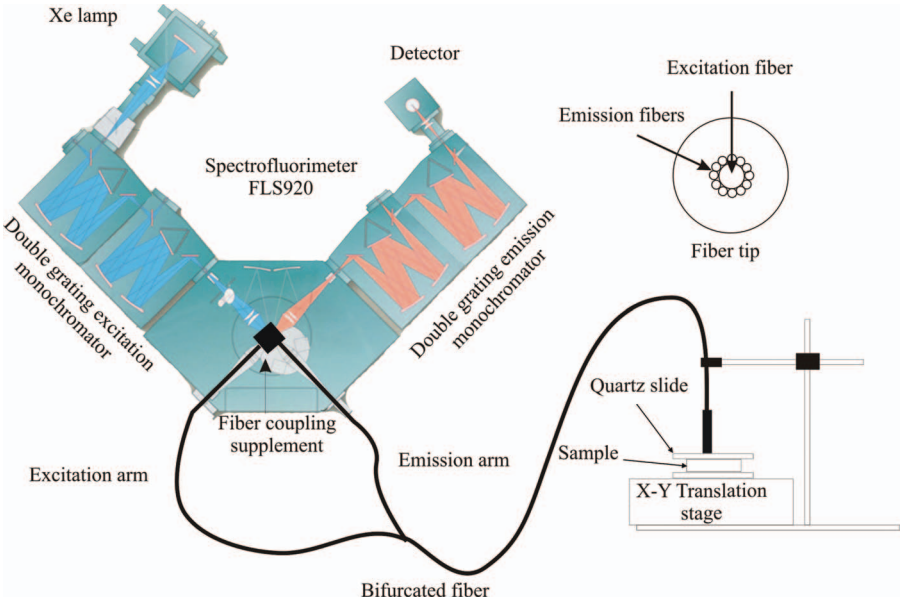

Fig. 2 The experimental setup and the fiber tip.

practice.[19] Histological slides were investigated with an optical microscope Olympus BX41. The pictures were taken with an attached microscopy camera Pixelink PL-A662.

The ninth heart tissue specimen that had not been examined previously was chosen to investigate the margins of HCS. The demarcation was performed in two ways: first by scanning the specimen along one line with high precision, and then by performing its planar scanning to test the applicability of the revealed spectral differences for the HCS visualization. During the precise linear scanning the distance between two investigated spots was 500 μm, while during the visual demarcation of HCS the planar area (11 mm $\times$ 15 mm) was scanned with the resolution of 1 mm. After the spectral measurements, four sections of the specimen were taken for histological analysis. One of the sections was taken along the scanning line and the rest were chosen randomly.

The autofluorescence spectra were measured by means of a spectrofluorimeter FLS920 (Edinburgh Instruments), Fig. 2. The instrument is equipped with a 450 W xenon lamp and a double grating monochromator to separate the appropriate wavelength for the fluorescence excitation. The detection arm is also equipped with a double grating monochromator and a thermoelectrically cooled photomultiplier tube. The excitation and the emission data are corrected for the instrument response automatically by factory preinstalled correction files. The special fiber coupling supplement (manufactured by Edinburgh Instruments) was installed in place of a standard cuvette holder in order to measure the fluorescence through a fiber bundle probe. The fiber probe (Avantes) enabled us to measure the spectra from particular places of the specimens. It was composed of a bundle of parallel quartz fibers: a central one (600 μm in diameter) for excitation and 12 (200 μm in diameter) being situated around the excitation fiber for the fluorescence detection. Typical excitation light intensity at the fiber tip was $\sim$ 50 μW.

The specimens were fixed between quartz slides and mounted on the *X*-*Y* translation stage. The thickness of the covering slide was 1 mm. A tip of the fiber was fixed in the holder and placed onto the slide surface. Different places of the specimen were selected for spectral measurements by translating the stage. It was assumed that the measurement conditions arranged in this manner had not changed for various spots of the same sample, thus allowing to compare the absolute intensities of the registered fluorescence spectra.

The significance of the difference has been evaluated in pairs between the fluorescence data of HCS and MC, as well as HCS and CT. The pair of MC and CT needed no evaluation due to intrinsic structural and obvious spectral differences. The testing within one specimen has been done using an independent t-Test. To test the significance of the difference between the fluorescence data from different specimens, a paired t-Test has been applied.

3 Results and Discussion

The fluorescence spectra of the heart tissues covered by the endocardium were registered on the preliminary marked places of the specimen. The spectral shapes and intensities were compared in order to determine the distinctive spectral region for selective HCS excitation. The apparent differences between the fluorescence spectra of the heart tissues were observed under excitation at 330 and 380 nm. Typical fluorescence spectra of HCS, CT, and MC registered on the same specimen of the heart through a layer of EC are presented in Fig. 3.

Similarly, as it was observed for the prepared endocardium free tissues,[17] the HCS covered by EC has the higher fluorescence intensity than MC under 330 or 380 nm excitation. CT has the higher fluorescence intensity than HCS when excited at 380 nm and the similar overall intensity when excited at 330 nm. It can be concluded that the excitation of the heart tissues at 330 nm results in the most apparent differences in spectral shape, while the excitation at 380 nm results in the highest differences in fluorescence intensity.

In ideal measurement conditions that were maintained for every specimen (see Sec. 2) HCS can be identified simply by

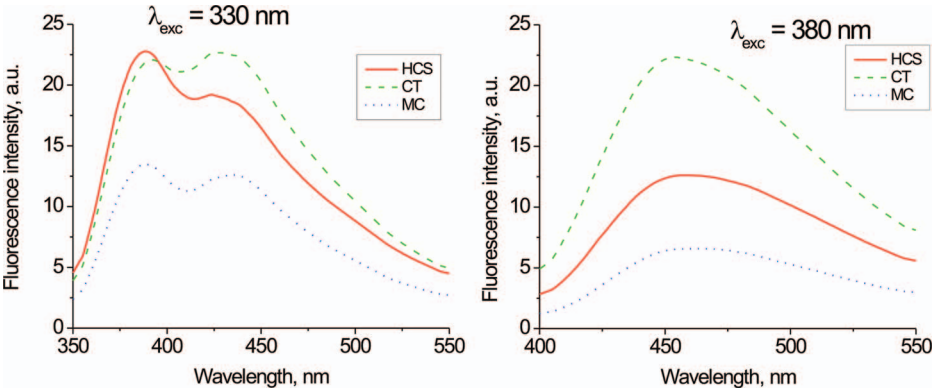

Fig. 3 Typical fluorescence spectra of HCS, CT, and MC. Spectra were measured on the same sample maintaining the same measurement conditions.

comparing the intensities of the tissue fluorescence. In the real situation, however, it is rather difficult to maintain the experimental conditions unaltered for every separate set of measurements. Alterations could result in different registered intensities of the tissue fluorescence even if the type of tissue would be the same. Nevertheless, when applying fluorescence spectroscopy for differentiation purposes, characteristic differences in the signal intensity that were revealed between the heart tissues as shown in Fig. 3 should be kept in mind. Moreover, these differences could be very useful for the direct optical imaging of the heart tissues. If the tissue is illuminated homogeneously during the visualization procedure, then the intensity of the fluorescence excitation will be the same for each point on the tissue. In such a case, those areas on the tissue that would distinguish itself by apparently different fluorescence intensities should be originated from different types of heart tissue.

Another spectral feature of the heart tissue specimens is the different shape of the fluorescence spectra registered under 330 nm excitation. As shown in Fig. 3, all fluorescence spectra of different types of the tissue registered under excitation at 330 nm are composed of two overlapping bands with peaks around 390 and 430 nm, which possess different intensity distributions. While the valley between the peaks is obviously the result of the remaining blood reabsorption, the relative intensities of the bands are different for all three types of heart tissue.

Our previous findings[17] revealed that there are no such bands in either fluorescence or fluorescence excitation spectra that would be specific for any type of heart tissue. This suggests that there is no specific fluorophore in HCS, CT, or MC. The electrophoresis studies that have been performed on tissue extracts[16] also revealed that HCS, CT, and MC contain similar proteins, but in different amounts. Consequently, the origin of the observed spectral differences is primarily the result of different amounts of collagen and elastin (330 nm is near an absorption peak of collagen, and 380 nm is mostly absorbed by elastin).[20] Since CT is rich in proteins—fluorophores such as collagen and elastin serving as structural elements in the heart the highest fluorescence intensity is observed for CT. MC is a muscular tissue and plays a key role in contracting the heart; therefore, it has only a small amount of structural proteins and the fluorescence intensity observed for the MC is considerably smaller than that for CT. The cells itself that form HCS also contain relatively small amounts of collagen and elastin, but the increased fluorescence intensity being comparable to that of CT could be due to the presence of the isolation shell made of collagen and elastin, which surrounds HCS cells and separates them from myocardium. The presence of an isolation shell is known to be around the His bundle and the Purkinje network;[8] therefore the fluorescence intensity should be similar for any of these HCS parts.

The differences detected in spectral shape and intensity imply that the highest contrast between different heart tissues during their spectral characterization should be obtained employing spectral properties of both collagen and elastin. Based on these findings the spectroscopic method is suggested for the differentiation of the HCS.

The main idea of the method is to excite autofluorescence at two different wavelengths and to register two intensity values in the region, where the differences between heart tissues are the biggest (400 to 500 nm, Fig. 3). The only limitation is the reabsorption of the fluorescence by blood that can significantly affect the measurement in living systems in the case of the presence of blood in the tissues. While it is hardly expected to happen during the actual cardiovascular operation procedure,[21] such a possibility cannot be completely neglected. Therefore, the registration region was selected around 460 nm, where the absorption of HbO_2 and Hb is minimal in the region of interest (Fig. 4).

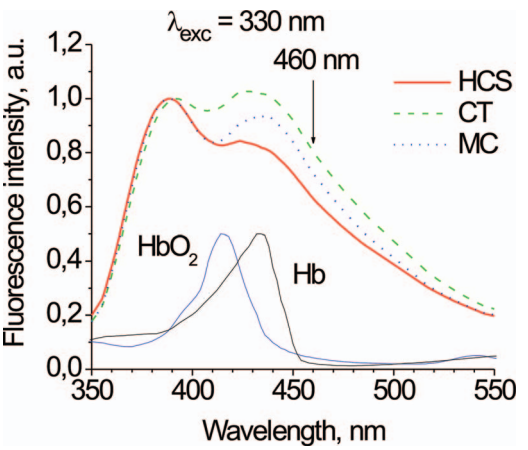

Fig. 4 Fluorescence spectra of HCS, CT, and MC normalized to the first band (at 390 nm). The normalized absorption spectra of HbO_2 and Hb are also added.

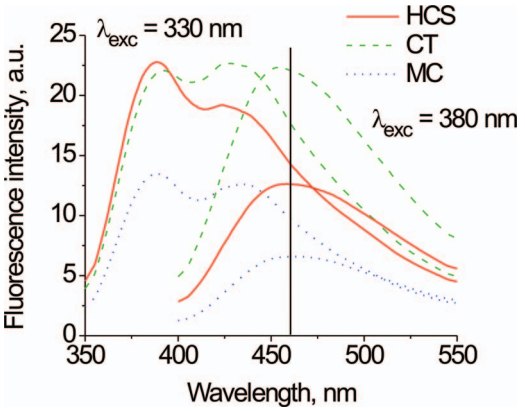

Fig. 5 Fluorescence spectra of HCS, CT, and MC tissues under 330 and 380 nm excitation. A vertical line marks 460 nm.

The relative changes in fluorescence intensity around 460 nm are different for different types of heart tissues under excitation in turn at 330 and 380 nm (Fig. 5). Such characteristic spectral features of the heart tissues could be exploited for differentiation purposes. Consequently, it should be possible to distinguish between three different types of heart tissues by a simple two-step procedure. First, registering fluorescence intensity twice only at one wavelength, 460 nm (instead of a whole fluorescence spectrum), under excitation at two wavelengths. Then, calculating the characteristic ratio of the intensities $I^{ex}{}_{330}(460)/I^{ex}{}_{380}(460)$ for the one measured spot and comparing it with the ratios calculated for other places of the specimen.

Such characteristic ratios $\langle R^{tiss}\rangle(460) = I^{ex}{}_{330}/I^{ex}{}_{380}$ were obtained in eight studied specimens at various spots that were preliminary attributed to different types of tissue. In some specimens the fluorescence intensity values were noticeably higher than in the others and the ratios obtained for the spots of these specimens were higher as well. The calculated ratios are summarized in Table 1. Table 1 also presents values of the significance levels $P(H_0 = 0)$ calculated for each of the eight specimens (in the case of MC) and for three of the eight specimens (in the case of CT). The significance of the difference between the ratios of the fluorescence intensities in the same heart specimen was verified using an independent t-Test for the null hypothesis ($\langle R^{HCS}\rangle - \langle R^{MC}\rangle \geq 0$, $\langle R^{HCS}\rangle - \langle R^{CT}\rangle \leq 0$).

The mean ratios $\langle R^{tiss}\rangle(460)$ obtained for each type of tissue were quite scattered comparing between different specimens (Table 1, values in columns 2, 4, and 6). Such variation is caused by the quantitative differences in the inner composition of the tissues in various hearts. Consequently, the averaged mean ratios had relatively large SD values: for HCS: 1.54 ± 0.58, for CT: 0.96 ± 0.14, and for MC: 2.23 ± 0.91 (Table 1, last row). Thus, the direct comparison between the ratios obtained in different specimens (hearts) is not suitable for practical application, as reflected, for instance, by increased SD of the averaged mean ratios in comparison with SD of the mean ratios being obtained for individual specimens.

On the other hand, the differences between the ratios of different heart tissues in the same specimen were found to be significant. As a rule, the mean ratio of the HCS was significantly higher than the ratio of CT and smaller than the ratio of MC (Table 1, values in rows). The statistical significance of such differences between the mean ratios of HCS and CT as well as HCS and MC for all studied specimens was evaluated by applying a paired t-Test for two samples and the same null hypothesis. The $P(H_0 = 0)$ value obtained for HCS and CT (0.025, three specimens) indicates that the chance of confusing HCS with CT in a randomly chosen heart specimen is less than 3%. The corresponding $P(H_0 = 0)$ value for HCS and MC (0.0031, eight samples) shows an even greater possibility to distinguish between these tissues on the basis of the obtained ratios.

Table 1 Fluorescence intensity ratios calculated at 460 nm under excitation at 380 and 330 nm.

Specimen	$\langle R^{CT}\rangle(460)$ ± SD (n)	$P(H_0 = 0) \times 10^{-3}$	$\langle R^{HCS}\rangle(460)$ ± SD (n)	$P(H_0 = 0) \times 10^{-3}$	$\langle R^{MC}\rangle(460)$ ± SD (n)
1			1.01 ± 0.03 (Ref. 3)	*6.9*	1.31 (Ref. 1)
2	0.92 ± 0.01 (Ref. 2)	*49.8*	1.14 ± 0.13 (Ref. 4)	*4.1*	1.60 ± 0.15 (Ref. 3)
3	1.12 (Ref. 1)	– [a]	1.64 (Ref. 1)	– [a]	1.94 (Ref. 1)
4	0.84 ± 0.04 (Ref. 2)	*17.2*	1.22 ± 0.09 (Ref. 2)	*26.3*	1.49 ± 0.01 (Ref. 2)
5			1.08 ± 0.1 (Ref. 3)	*1.28*	2.16 ± 0.16 (Ref. 2)
6			1.85 ± 0.02 (Ref. 2)	*21.5*	2.23 (Ref. 1)
7			2.75 ± 0.02 (Ref. 2)	*12.7*	3.98 ± 0.28 (Ref. 2)
8			1.59 ± 0.02 (Ref. 2)	*5.35*	3.14 (Ref. 1)
Averaged mean ratio	**0.96 ± 0.14 (Ref. 5)**	***(25.0)***	**1.54 ± 0.58 (Ref. 19)**	***(3.10)***	**2.23 ± 0.91 (Ref. 13)**

$\langle R^{CT}\rangle$, $\langle R^{HCS}\rangle$, and $\langle R^{MC}\rangle$: mean values of the corresponding ratios of the same sample.
SD: standard deviation.
(n): represents the number of measurement points.
$P(H_0 = 0)$ – values of significance levels for the null hypothesis ($\langle R^{HCS}\rangle - \langle R^{MC}\rangle \geq 0$, $\langle R^{HCS}\rangle - \langle R^{CT}\rangle \leq 0$) .
[a]The $P(H_0 = 0)$ value could not be calculated because the difference of the standard error is 0. However, at the 0.05 level, the two values are significantly different.

Table 2 Values of the fluorescence intensity ratios calculated at 460 nm under excitation at 330 and 380 nm and normalized to the ratio of HCS in the same sample.

Number of specimen	$\langle R^{CT}{}_n\rangle(460)$	Confidence interval	$\langle R^{HCS}{}_n\rangle(460)$	Confidence interval	$\langle R^{MC}{}_n\rangle(460)$
1			*1 ± 0.03*		*1.3*
2	*0.81 ± 0.01*		*1 ± 0.11*		*1.40 ± 0.13*
3	*0.68*		*1*		*1.18*
4	*0.69 ± 0.03*		*1 ± 0.07*		*1.22 ± 0.01*
5			*1 ± 0.09*		*2.00 ± 0.15*
6			*1 ± 0.01*		*1.21*
7			*1 ± 0.01*		*1.45 ± 0.1*
8			*1 ± 0.01*		*1.97*
Averaged	***0.73 ± 0.07***	**0.15**	***1 ± 0.11***[a]	**0.24**	***1.47 ± 0.33***

$\langle R^{CT}{}_n\rangle$, $\langle R^{HCS}{}_n\rangle$ and $\langle R^{MC}{}_n\rangle$: mean ratios of the corresponding tissue normalized to the $\langle R^{HCS}\rangle$ value of the same sample.
[a]The maximal standard error value has been taken.

Thus, the obtained findings support the possibility of distinguishing the HCS from the other types of heart tissue by calculating these ratios in a particular specimen. However, the proposed method for tissue comparison can be modified taking into account the aforementioned individual variations observed between the hearts.

For that, all ratios in each specimen were normalized to the mean ratio of HCS for that specimen. The obtained normalized mean values $\langle R^{tiss}{}_n\rangle(460) = \langle R^{tiss}\rangle(460)/\langle R^{HCS}\rangle(460)$ are shown in Table 2. This normalization provides the additional possibility to calculate the confidence intervals for the obtained normalized ratios. The confidence intervals were calculated with a significance level of 0.05. For instance, in the case of HCS and CT "0.15" indicates that $R^{tiss}{}_n(460)$ higher than 0.85 can be attributed to HCS. On the other hand, in the case of HCS and MC "0.24" indicates that $R^{tiss}{}_n(460)$ higher than 1.24 does not belong to HCS and could be attributed to MC. Thus, the obtained confidence interval $0.85 < R^{tiss}{}_n(460) < 1.24$ determines the heart tissue, which on the basis of the spectral properties can be attributed to HCS with 95% probability. It has to be noted that this confidence interval was not exceeded by any of the experimentally obtained ratios.

Acquired results imply that during differentiation of the HCS the registered fluorescence intensities should be recalculated for every specimen (or a heart) by normalizing registered ratios to the value from a clearly recognizable site of HCS in the tissue, and then the normalized ratios should be used for differentiation between the tissues in the rest of the heart.

On the other hand, if it is not possible to find a plausible HCS location in the heart during the surgery procedure, the tissue differentiation could be started by measuring reference values from MC. In this case the averaged $\langle R^{MC}{}_n\rangle$ value is also needed (Table 2). $\langle R^{MC}{}_n\rangle(460)$ value of 1.47 being calculated from eight specimens (hearts) indicates how much the ratio of the MC is expected to be higher than the ratio of the HCS in the same heart. This number can be assigned as a reference value V_{MC}. In order to ensure a higher reliability, this value obviously should be calculated from the higher number of specimens. Then, the HCS ratio could be calculated in the following way: $\langle R^{HCS}\rangle(460) = \langle R^{MC}\rangle(460)/V_{MC}$, where $\langle R^{MC}\rangle$ is the average of the measured reference values from MC. For example, in specimen (heart) No. 2, the ratio $\langle R^{tiss}\rangle(460)$ measured from MC is 1.6. The calculated ratio of HCS for specimen No. 2 is: $\langle R^{HCS}\rangle(460) = 1.6/1.47 = 1.09$. The upper and lower limits of the HCS ratio can also be evaluated from the corresponding confidence intervals (Table 2). Since these intervals were calculated for the ratios normalized to the HCS ratio, these values should be multiplied by $\langle R^{HCS}\rangle(460)$; in our example—by 1.09. The lower limit representing the value, below which the tissue could be attributed to CT, is: $\langle R^{HCS}\rangle(460) - (0.15*1.09) = 0.93$. The upper limit representing the value, above which the tissue could be attributed to MC, is: $\langle R^{HCS}\rangle(460) + (0.24*1.09) = 1.35$. These limiting values indicate that in specimen No .2, the tissue possessing the measured ratios $R^{tiss}(460)$ between 0.93 and 1.35 could be attributed to the HCS with the probability of 95%. This interval shows good coincidence with experimentally obtained data for HCS (1.14 ± 0.13, Table 1). In fact, both ratios of other tissues (0.92 ± 0.01 for CT, 1.60 ± 0.15 for MC) present in this specimen were out of the calculated interval.

The fluorescence spectra have also been measured on random spots in places of specimens that were not marked by the pathologist. It has to be noted that there were intensity ratios calculated for some of those spots that corresponded to neither type of tissue on a specimen. We suppose that this could be due to the diameter of the fibers in the bundle that were used for fluorescence excitation (0.6 mm) and detection (0.2 mm). Possibly in those spots the tip could have touched the specimen in between different heart tissues and the fluorescence spectra recorded on such spots represented the combination of the fluorescence emerging from these tissues. As a result, the values of the ratios were somewhere in between those representing the marked places that were attributed to one type or the other type of the tissue on a particular specimen. Due to unclear origin of the fluorescence the ratios of these spots were not included

in the subsequent calculations of the means and the standard error values, presented in Tables 1 and 2. In order to clarify the appearance of ambiguous points, the fluorescence measurement has been performed through the entire branch of HCS.

The precise spectroscopic demarcation of HCS boundaries was demonstrated on the ninth tissue specimen by performing the linear scanning. The specimen as it looked in the daylight is presented in Fig. 6(a) and the image of the specimen under 365 nm illumination is presented in Fig. 6(b). Like in the previous experiments, the fluorescence was excited at each spot in turn at 330 and 380 nm and the fluorescence intensity was registered at 460 nm. Four lines (1–4) in Fig. 6(b) represent the sections, where the histological analysis was carried out. The heart tissue images representing the histological section of scanning line No. 2 is shown in Fig. 7. The location of the HCS in each section is marked by the dashed part of the line [Fig. 6(b)]. The solid part of the line corresponds to the MC tissue. The stars mark the location of CT, which was found only in one section (section 4).

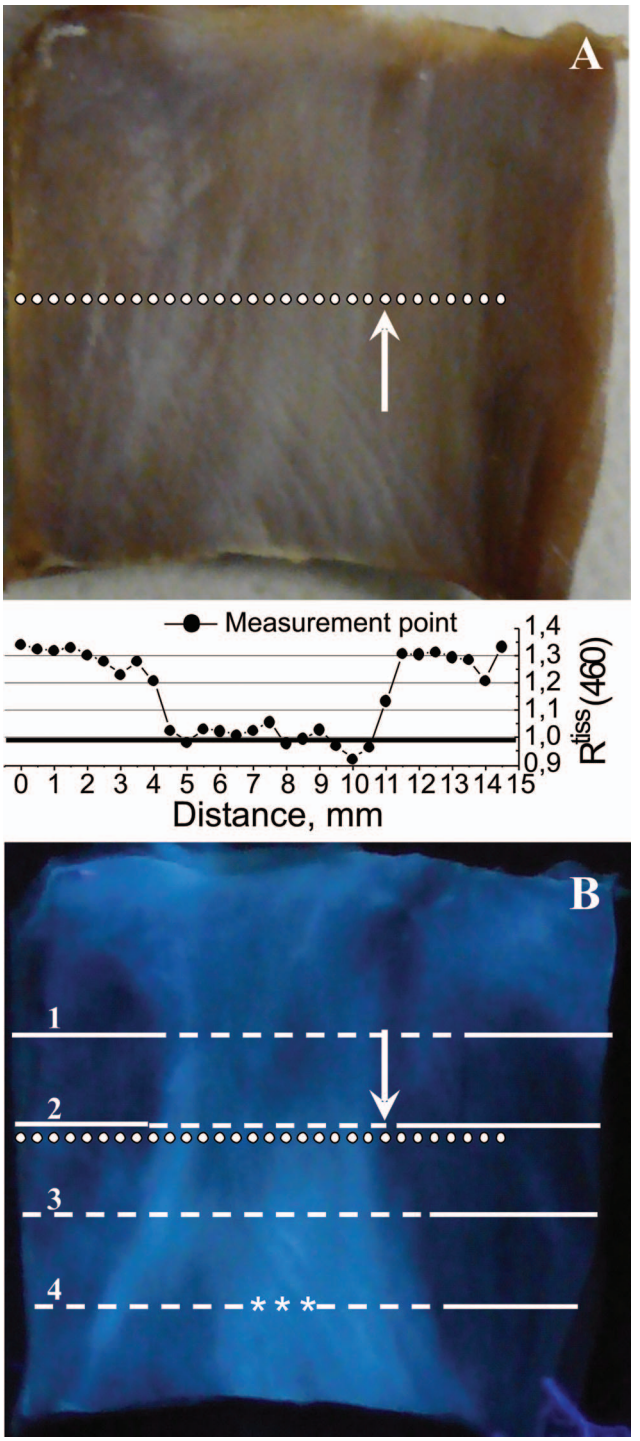

Fig. 6 Linear scanning of the sample. (a) The image of the specimen in the daylight. Points where the ratios were measured along the line are marked by dots. (b) The image of the same specimen under irradiation of an Hg lamp at 365 nm. The ratios $R(460) = I^{ex}{}_{330}/I^{ex}{}_{380}$ calculated for each spot are presented between the images.

The direct correlation has been observed between the different ratios $R^{tiss}(460) = I^{ex}{}_{330}/I^{ex}{}_{380}$ calculated for the spots lying along the line of scanning and the areas possessing different fluorescence intensities that are visible in the fluorescence image [Fig. 6(b)]. The ratio $R^{tiss}(460)$ from the histologically confirmed HCS area (the dashed part of the histological section No. 2) is around 1. Since there was no histologically confirmed CT along section line 2, points with $R^{tiss}(460)$ values around 1.0 could be attributed to HCS. No normalization to HCS value has been done in this case. It should be noted that there were also two other specimens that had $\langle R^{HCS}\rangle(460)$ values around 1 (Table 1). The ratio $R^{tiss}(460)$ from the histologically confirmed MC area (solid parts of the histological section No. 2) is around 1.3.

Also, there was a spot [$R^{tiss}(460)$ value around 1.15], which, as mentioned above, corresponded to neither type of the tissue—judging from the fluorescence image of the specimen and the histological analysis (Fig. 7)—it was located on the edge between two different types of tissue (shown by an arrow in Figs. 6 and 7 pictures). These data confirm the possible cause of the ambiguous points. However, as it is seen in Fig. 6, such a situation causes a minor practical problem, since it could be solved simply by measuring fluorescence just parts of the millimeter away from an equivocal spot.

The data of the linear scanning suggest that all regions in the specimen, where the intensity ratio is around 1.3, could be assigned to MC. In addition, there were no $R^{tiss}(460)$ values detected lower than 0.9 during the linear scanning. Based on the scanning results the ratio for CT in this specimen is expected to be less than 0.9. These experimentally detected limits again

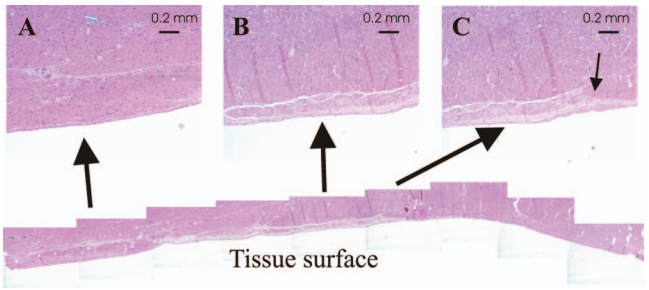

Fig. 7 Histological images of the section No. 2. (a) Shows the ordinary MC covered by a thin layer of EC. (b) Shows a branch of HCS close to the tissue surface. The branch consists of muscular bundles with Purkinje fibers surrounded by CT. (c) Shows the boundary of the HCS branch that is marked by an arrow.

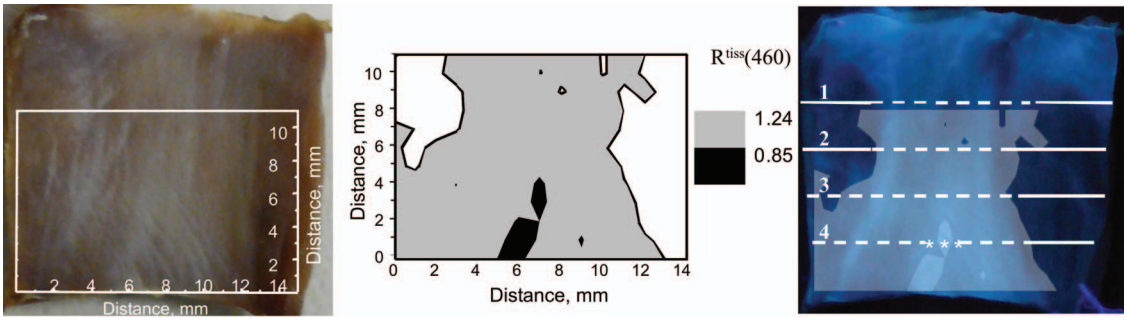

Fig. 8 Planar scanning of the specimen. Picture in the daylight (left panel); spectral image (middle panel); combined picture of spectral and fluorescence images (right panel). Four lines in the right image mark sections of the sample taken for histological studies.

show good coincidence with the limiting values that could be calculated from the confidence intervals (Table 2). In this specimen $\langle R^{HCS}\rangle(460) \approx 1.00$, therefore the lower limiting value for HCS is $1.00 - [0.15\times\langle R^{HCS}\rangle(460)] = 1 - 0.15 = 0.85$. The upper limiting value for HCS is $1.00 + [0.24\times\langle R^{HCS}\rangle(460)] = 1.00 + 0.24 = 1.24$. The slight variations of the ratio values detected for the spots attributed to the HCS (Fig. 6) could be caused by a fibrous microstructure of the HCS, which produced an uneven fluorescence intensity under the tip of the optical fiber. The single HCS fibers cannot be resolved due to the limited spatial resolution, therefore it appears as the broad HCS branch. A thin Purkinje network that appears in the ventricles will elevate the detected background signal of the endocardium.

The applicability of the revealed spectral differences for the visualization of the HCS tissue was demonstrated by the planar scanning of the same specimen. In this case the spectral image was obtained, each point of which corresponded to the calculated value of the ratio $R^{tiss}(460) = I^{ex}{}_{330}/I^{ex}{}_{380}$. The boundaries of the scanned area are marked on the daylight picture (Fig. 8). Based on the data from the linear scanning and the confidence intervals, the area that possessed $0.85 < R^{tiss}(460) < 1.24$ was attributed to HCS with a probability of 95%. The digital spectral image was then overlaid on the photograph of the sample illuminated at 365 nm (Fig. 8). As it is seen on the combined picture, the tissue area that was marked by ratio values in the range of 0.85 to 1.24 closely overlaps with the fluorescing area visible on the image. Slight variations of the boundaries could be due to the limited scanning resolution. Spectral scanning also revealed the area of the specimen where $R^{tiss}(460)$ was lower than 0.85. This area is marked black in the digital picture (middle panel, Fig. 8). According to the spectral analysis it should be attributed to CT. The subsequent histological analysis of the tissue confirmed the presence of the CT in the central part of section 4.

4 Conclusions

In conclusion, the proposed spectroscopic method allows to differentiate the conduction system of the human heart from surrounding heart tissues but it does not allow to distinguish between distinct tissue types of the conduction system itself. The limited spatial resolution restricts the detection capacity to the thicker HCS strands and does not allow to identify the thin Purkinje network that would elevate the detected background signal of endocardium.

While this paper presents only the principles of the methods, good coincidence of the spectral and fluorescence images with histological data so far seem encouraging in the view of the possibility to apply the fluorescence methods for the differentiation or visualization of HCS during clinical surgery. In the areas of the heart, where the presence of pure CT is minimal, the additional illumination at 365 nm could be applied in order to estimate the boundaries of the HCS. For more confusing places of the heart, the more precise evaluation based on the proposed ratio analysis could be employed. However, since all the experiments were performed *ex vivo* and the real conditions were only envisaged, further experiments are planned on a nonfixed heart specimen.

Acknowledgments

The authors gratefully acknowledge the financial support provided to this study by the Lithuanian Science Council under Grant No. LIG-25/2010.

References

1. B. M. Cullum, "Fluorescence spectroscopy for biomedical diagnostics," in *Biomedical Photonics Handbook*, T. Vo-Dinh, Ed., V. Biomedical Diagnostics II Optical Biopsy, CRC Press, Orlando, Florida (2003).
2. R. Rotomskis, "Optical biopsy of cancer: nanotechnological aspects," *Tumori* **94**(2), 200–205 (2008).
3. P. P. Karpawich, "Pacemaker therapy in the postoperative patient," *Turkish J. Arrhythmia, Pacing and Electrophysiology* **1**(3), Supplement 1, 48–52 (2003).
4. Z. Emkanjoo, M. Mirza-Ali, A. Alizadeh, S. Hosseini, M. V. Jorat, M. H. Nikoo, and M. A. Sadr-Ameli, "Predictors and frequency of conduction disturbances after open heart surgery," *Indian Pacing Electrophysiology J.* **8**(1), 14–21 (2008).
5. G. Limongelli, V. Ducceschi, A. D'Andrea, A. Renzuli, B. Sarubbi, M. De Feo, F. Cerasuolo, R. Calabrò, and M. Cotrufo, "Risk factors for pacemaker implantation following aortic valve replacement: a single centre experience," *Heart* **89**(8), 901–904 (2003).
6. R. H. Anderson, J. Yanni, M. R. Boyett, N. J. Chandler, and H. Dobrzynski, "The anatomy of the cardiac conduction system," *Clin. Anat.* **22**(1), 99–113 (2009).
7. J. Langman and M. W. Woerdeman, *Atlas of Medical Anatomy*, The Saunders Press, Philadelphia (1982).
8. "Development of the cardiac conduction system," *Symposium on Development of the Cardiac Conduction System*, held at the Novartis Foundation, London, May 21–23, 2002.
9. M. D. Silver, *Cardiovascular Pathology*, p. 1367, Churchill Livingstone, New York (1991).
10. E. Žurauskienė, E. Žurauskas, G. Streckytė, S. Bagdonas, K. Žvaigždinas, and R. Rotomskis, "Premises of visualization of the con-

duction system of heart: spectroscopic investigations," *Lith. J. Phys.* **41**, 505–508 (2001).
11. P. M. Larionov, A. N. Malov, M. M. Mandrik, N. A. Maslov, and A. M. Orishich, "Changes in the laser-induced fluorescence spectrum of myocardium tissue with decrease in its viability," *J. Appl. Spectrosc.* **70**(1), 38–42 (2003).
12. M. Perk, G. J. Flynn, S. Gulamhusein, Y. Wen, C. Smith, B. Bathgate, J. Tulip, N. A. Parfrey, and A. Lucas, "Laser induced fluorescence identification of sinoatrial and atrioventricular nodal conduction tissue," *PACE* **16**, 1701–1712 (1993).
13. G. E. Kochiadakis, S. I. Chrysostomakis, M. D. Kalebubas, G. M. Filippidis, I. G. Zacharakis, T. G. Papazoglou, and P. E. Vardas, "The role of laser-induced fluorescence in myocardial tissue characterisation," *Chest* **120**, 233–239 (2001).
14. A. M. K. Nilsson, D. Heinrich, J. Olajos, and S. Andersson-Engels, "Near infrared diffuse reflection and laser-induced fluorescence spectroscopy for myocardial tissue characterisation," *Spectrochim. Acta, Part A* **53**, 1901–1912 (1997).
15. L. Marcu, W. S. Grundfest, and M. C. Fishbein, "Time-resolved laser-induced fluorescence spectroscopy for staging atherosclerotic lesions," in *Handbook of Biomedical Fluorescence*, pp. 397–430, M. A. Mycek and B. W. Pogue, Eds., Marcel Dekker, Inc., New York (2003).
16. J. Venius, D. Labeikytė, E. Žurauskas, V. Strazdaitė, S. Bagdonas, and R. Rotomskis, "Investigation of human heart tissue extracts by spectroscopic methods," *Biologija* **3**, 53–58 (2006).
17. S. Bagdonas, E. Zurauskas, G. Streckyte, and R. Rotomskis, "Spectroscopic studies of the human heart conduction system ex vivo: implication for optical visualization," *J. Photochem. Photobiol., B* **92**(2), 128–34 (2008).
18. E. Žurauskas, S. Bagdonas, L. Bandzaitytė, G. Streckytė, and R. Rotomskis, "Visualization of the conduction system of heart by fluorescence spectroscopy," *Lith. J. Phys.* **44**, 35–40 (2004).
19. J. D. Bancroft and M. Gamble, *Theory and Practice of Histological Techniques*, 725 p., Elsevier Health Sciences, Philadelphia (2008).
20. G. A. Wagnieres, W. M. Star, and B. C. Wilson, "In vivo fluorescence spectroscopy and imaging for oncological applications," *J. Photochem. Photobiol.* **68**, 630–632 (1998).
21. H. J. Geissler and U. Mehlhorn, "Cold crystalloid cardioplegia," *Multimedia Manual of Cardiothoracic Surgery* (2006).